 doi:10.20944/preprints202209.0081.v1

Article

Microstructure and Cyclic Oxidation Resistance of Ce-Si Modified Aluminide Coating Deposited by Pack Cementation on Inconel 738LC

Parviz Nourpoor[1], Soheila Javadian [1,*], Alireza Sabour Rouh Aghdam[2] and Farzin Ghadami[2]

[1] Department of Physical Chemistry, Faculty of Science, Tarbiat Modares University, P.O. Box:14115-143, Tehran, Iran
[2] Department of Materials Engineering, Faculty of Engineering, Tarbiat Modares University, P.O. Box:14115-143, Tehran, Iran
* Correspondence: javadian_s@modares.ac.ir; Fax: +98-21-82883455

Abstract: The synergistic effect of silicon and cerium addition on the oxidation resistance of pack cementation aluminide coating applied on Ni-based superalloy substrate was investigated. The effect of cerium and silicon on the scale morphology, oxidation behavior, and scale spallation tendency are discussed based on the experimental results, using X-ray diffraction (XRD), scanning electron microscopy (SEM), and energy-dispersive X-ray analyses (EDX). In addition, the oxidation resistance was evaluated by measuring the weight of samples after each 16-hour cycle at 1100°C for 50 cycles. The experiments indicated that silicon addition to aluminide coating improves the oxidation resistance through the formation of β-NiAl1-nSin and δ-Ni2Al3-nSin and δ-Ni2Si phases. Furthermore, the addition of 1% cerium to modified aluminide enhances the formation of the fine-grained microstructure of the β-NiAl and δ-Ni2Al3 and reduces the outward/inward diffusion of elements (so-called blocking effect) which significantly modifies the hot oxidation resistance. The addition of 2% cerium, owing to the distortion of the β-NiAl and δ-Ni2Al3 phases, strictly decreases the hot oxidation resistance and the coating is exfoliated after 450 h at 1100 °C. The cyclic oxidation tests showed that the samples containing 1% cerium and 6% silicon possess the highest hot oxidation resistance in which 2 mg/cm2 weight loss of Ce-Si-aluminide was reported after 800 h. This is attributed to the simultaneous effect of cerium and silicon during the deposition process which reduces the oxygen diffusion and reduces the growth rate of α-Al2O3 during oxidation tests. The α-Al2O3 oxidation layer morphology showed that finer grains are formed in samples containing optimum ratios of cerium and silicon which indicates that these elements improve the coating adhesion and oxidation resistance simultaneously.

Keywords: pack cementation; Ce-Si modified aluminide coating; cyclic oxidation resistance

1. Introduction

High-temperature oxidation and corrosion inevitably occur in the aggressive environment of gas turbine engines which are applied in aircraft, aerospace, navy, gas and oil industries and power generation units. Nickel-based superalloys due to their excellent mechanical strength and creep resistance at high temperatures are widely used in the critical hot section of gas turbines such as combustion chambers, turbine stators, and rotors [1,2]. However, Nickel-based superalloys are not able to provide significant resistance against high-temperature oxidation and hot corrosion during long-time exposure. Thus, the appropriate coating has to be applied to enhance the high-temperature oxidation and hot corrosion resistance of the nickel-based superalloys [3,4]. Thermal barrier coating (TBC), MCrAlY overlays, and diffusion aluminides coatings are promising candidates to protect the surface at high temperatures [5-8]. TBC coatings provide thermal insulation and thus lower the temperature of the metallic substrate by virtue of its thermal conductivity. Thus, those are currently applied in the hot section parts at operational

 doi:10.20944/preprints202209.0081.v1

temperatures higher than 1100 ˚C which need complicated and expensive technologies [5,6,9-11]. Versatile and cost-effective conventional aluminide diffusion coatings usually protect the hot section parts at lower temperatures like the low-pressure turbine (LPT) section at 700-1100 ˚C temperature range in the gas turbines [12-14]. Nowadays, modified aluminide diffusion coatings are investigated to improve the durability of hot section parts in gas turbines working at high temperatures [15-19]. The modified aluminide coatings improve the gas turbine performance by increasing turbine inlet temperature (TIT) and prolong the time between overhauls (TBO) of them [20,21]. Conventional aluminide coatings have been modified by adding beneficial elements such as chromium, silicon, cobalt, and platinum [17,22-25] or by doping reactive elements (REs), e.g., hafnium, zirconium, cerium, lanthanum, yttrium, and other REs by using numerous techniques such as pack cementation, chemical vapor deposition (CVD), slurry, or co-diffusion methods [26-34]. Nonetheless, the addition of silicon into conventional aluminide coatings enhances the resistance against carburization, hot corrosion, and high-temperature oxidation [16,35,36]. On the other hand, the high silicon content has negative side effects on the mechanical performance of the coating resulting in cracking and spallation. The problem of cracking and spallation in Si-modified aluminide coatings could be overcome using the optimum silicon reservoir phase [37,38] and REs contents doped in the coatings[39]. Cerium has a high affinity toward oxygen a large atomic radius compared to nickel, aluminum, chrome, cobalt, and low solid solubility in β-NiAl phases [15,40]. The optimized amount of cerium and cerium oxides deposited in the scale/coating interface and along grain boundaries leads to improvement of the lifetime and thermal stability of the aluminide coatings. The optimized content of segregated cerium ions inhibits the rapid outward/inward intermetallic diffusion of elements along the coating grain boundary and cause a finer-grained microstructure of the β-NiAl and δ-Ni_2Al_3 phases in the coatings [41,42] which enhances the oxide scales adhesion, hot corrosion, and oxidation resistance of the aluminide coating [33,43-46]. Cerium mostly stands against the outward diffusion of aluminum ions and inward diffusion of oxygen through the process named ‘‘the blocking effect”. It is responsible for the reduction of the alumina scale growth rate on the surface of the coating [29,41,47]. Moreover, cerium or its oxides to heat-resisting alloys significantly increases the adherence of $A1_2O_3$ and Cr_2O_3 scales when silicon was present in the alloy [48].On the contrary, the high content of cerium in the coating diffuses into the solid solution and increases the energy of the system by distortion and mismatch of the β-NiAl lattice. Thus, high cerium content diminishes resistance against hot corrosion and oxidation because of the rising rate of spallation and rumpling of the aluminide coatings [15].

In recent years, the addition of two beneficial elements to the conventional aluminide coating has been researched to overcome the above problems [15,16,27,29,34,49-51]. The synergistic Ce-Si addition effect on the high-temperature oxidation behavior of the modified aluminide coatings is not yet investigated in detail. So, in the present work, the influence of Ce and Si on the high-temperature oxidation behavior of the aluminide coatings applied by the pack cementation process has been investigated. In this regard, the different combinations of cerium and silicon amounts were comprehensively examined to find the optimized Ce-Si-modified aluminide coating. Then, the diffusion mechanism, properties, and synergism of contributing aluminum, silicon, and cerium elements were investigated through microstructural characterization as well as high-temperature oxidation properties. Finally, the optimum composition of the mentioned additive elements in the modified aluminide coating was determined.

2. Materials and Methods

2.1. Substrate materials and preparation

The cast Ni-base superalloy IN738LC with the composition of bal. Ni, 8.5%Co, 16%Cr, 3.4% Ti, 2.6% W, 1.75% Ta, 3.4% Al, 1.7% Mo, 0.9%Mo (%wt) was used as the substrate. The specimens were sliced into squares with dimensions of 20×20×2 mm by

Preprints (www.preprints.org) | NOT PEER-REVIEWED | Posted: 6 September 2022 doi:10.20944/preprints202209.0081.v1

using wire-electrode cutting. The surface and the sides of all specimens were carefully ground with 800-grit SiC emery paper.

2.2. Coating procedure

Regarding the deposition of the coatings using the pack cementation method, the substrate samples were degreased and cleaned in an ultrasonic bath containing acetone for 30 min and finally put into cementation pack boxes. Commercial pure powders of aluminum, silicon, $CeCl_3$, Al_2O_3, and NH_4Br (≥99.9% grade) with average particle sizes of all less than 270 mesh were then used as the main precursors of the pack cementation process. In this case, the ammonium bromide activator was used to promote the formation of halide gases of aluminum, silicon and cerium to their diffusion into the substrate during the pack cementation process. The specimens were buried in the uniform pack powder in a cylindrical steel retort following the procedure reported elsewhere [52]. The retorts were heated to 1000°C at a flow rate of 6 C.min-1 and kept for 2 h. In order to investigate the effect of cerium on the properties of coatings, three different contents of cerium were used listed in Table 1. Based on the oxidation resistance of coatings, optimized cerium content (1%$CeCl_3$≡ %0.76Ce) was selected. Then, according to Table 1, three different contents of silicon are changed in order to trace its effect on the properties of coatings.

Table 1. Composition of pack mixture for applying aluminide coatings*.

Sample	Code	Content of composition (wt.%)			
		Al	Si	CeCl3	NH4Br
No. 1	Ce0Si3	6	3%	0	2.0
No. 2	Ce1Si3	6	3%	1%	2.0
No.3	Ce2Si3	6	3%	2%	2.0
No.2	Ce1Si3	6	3%	1%	2.0
No.4	Ce1Si0	6	0%	1%	2.0
No.5	Ce1Si6	6	6%	1%	2.0

* Total content of pack mixture was measured as 60 g.

2.3. Microstructural characterization

Scanning electron microscopy (SEM, Philips-XL30) was used to analyze the microstructure by examining the cross-section and surface of the coatings. The elemental composition and microstructure of the coatings were determined using element mapping (MAP) by using an energy dispersive spectrometer (EDS). The surface phase composition of the coatings was then investigated by X-ray diffraction (XRD, Philips X'Pert MPD) using Cu Kα radiation (1.5418 Å) at 40 kV and 40 mA. A low scanning rate of 0.02°/s was used to obtain the desired precision.

2.4. Cyclic oxidation tests

The evaluation of the hot oxidation resistance of the coatings has been carried out by using weight change measurements during cyclic heating in air. The samples were ultrasonically cleaned in acetone, rinsed and dried. The prepared samples were weighed with a balance of 0.1 mg precision and placed on an aluminide ceramic pan for oxidation tests. All samples were placed in a furnace and examined under oxidation at 1100 °C during 50 cycles where each cycle equals 16 h (Fig. 1) and weight variations were recorded. The weight change per unit surface area was determined after each oxidation cycle. Finally, the surface of the samples was investigated by using SEM and XRD to characterize the surface properties of the coating.

Preprints (www.preprints.org) | NOT PEER-REVIEWED | Posted: 6 September 2022 doi:10.20944/preprints202209.0081.v1

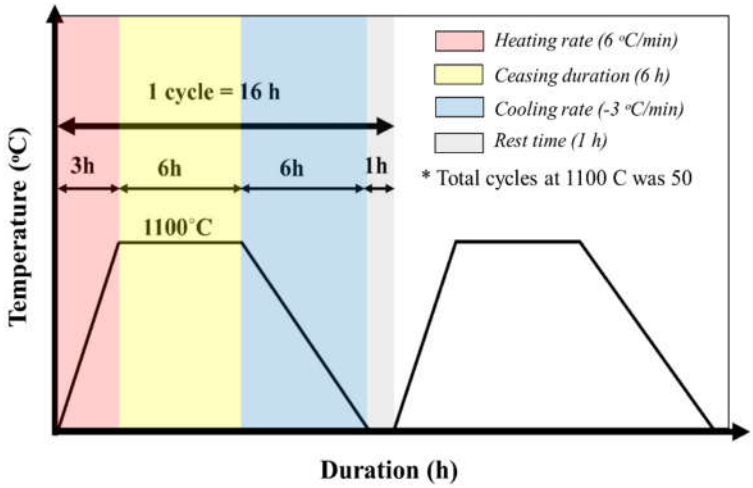

Figure 1. The hot cyclic oxidation test diagram which carried out on coated samples.

3. Results and discussion

3.1. Microstructure of Al-Si-Ce coatings

In order to investigate the diffusion mechanism of Al-Si-Ce pack cementation, the samples Ce0Si3, Ce1Si0, and Ce1Si6 were characterized by using the SEM-EDX method which is shown in Fig. 2 and Table 2. According to Fig. 2, the coatings reveal a thickness between 40-50 μm. In addition, the coating cross-section shows its regions including two layers: the outer layer of ~35-45 μm thick and the diffusion zone of ~3-5 μm. The diffusion zone indicates that the formation of coating is based on high-temperature low activity aluminizing (known as HTLA) coating type which is primarily attributed to the outward Ni, Cr, and Co diffusion. Thus, in comparison to inward aluminum, silicon and cerium diffusion, the outward substrate elements like Ni, Cr, Co, etc. diffusion is scale-up in the HTLA Pack cementation process.

Preprints (www.preprints.org) | NOT PEER-REVIEWED | Posted: 6 September 2022 doi:10.20944/preprints202209.0081.v1

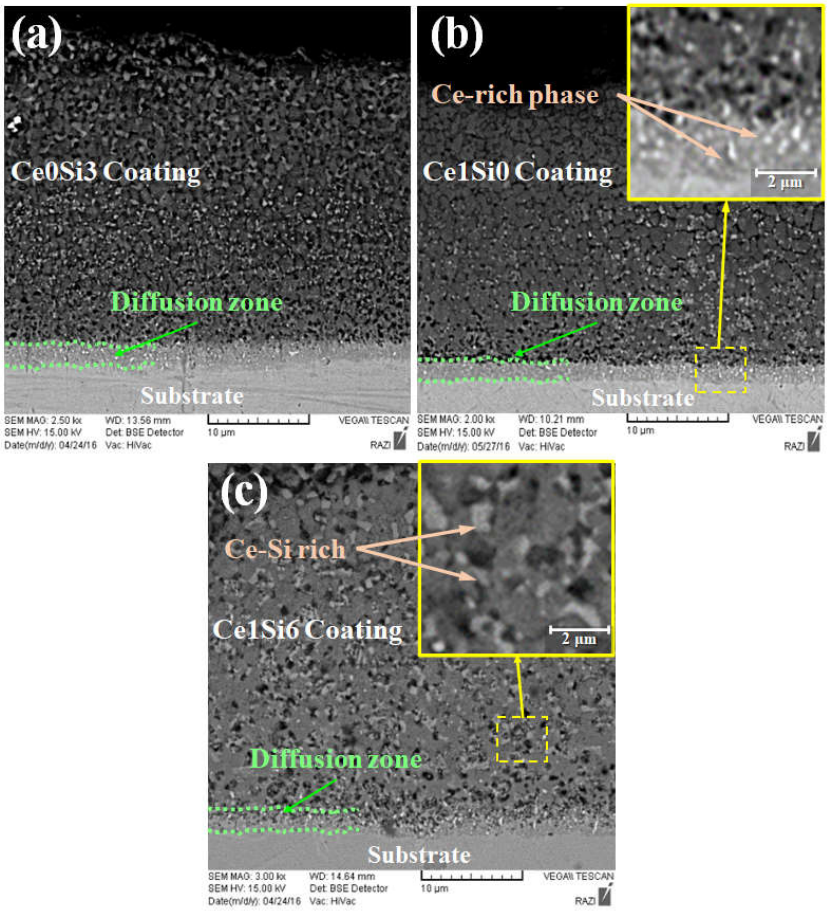

Figure 2. Cross-sectional image micrograph of the modified aluminized coatings consisting of two distinguished layers, a) Ce0Si3, b) Ce1Si0, and c) Ce1Si6.

According to Table 2, which shows the composition of part A in the coatings, it shows the low rate of diffusion of cerium to the substrate according to its large radius in comparison with nickel and aluminum.

Table 2. Elemental percentage (wt.%) on the selected samples by EDX analysis.

Elements	Ce0Si3	Ce1Si3	Ce2Si3	Ce1Si0	Ce1Si6
Ni	34.80	41.67	42.66	54.49	41.86
Cr	9.86	11.06	10.61	1.34	11.82
Co	4.00	5.53	6.2	5.28	4.87
Al	46.90	38.63	33.67	32.25	37.51
Si	1.37	0.38	0.25	0.01	1.03
Ce	0.01	0.70	0.93	0.75	0.66

The cerium's large atomic radius causes a low diffusion rate to the substrate in the pack cementation process [15]. According to Fig. 3, the raising of Nickel and decreasing of Al and Si concentration are shown as scale in coatings. It can be attributed to the HTLA effect which reduces the aluminum and silicon diffusion inside the superalloy. Also, cerium mainly is placed into the grain boundary of β-NiAl and δ-Ni2Al3 phases since its greater radius compared to nickel and aluminum (the radius of cerium, nickel, and aluminium are 0.185, 0.135 and 0.125 nm, respectively) and its effect to increase the energy of the system. Thus, cerium firstly is replaced in grain boundaries and Scale/alloy interface

Preprints (www.preprints.org) | NOT PEER-REVIEWED | Posted: 6 September 2022 doi:10.20944/preprints202209.0081.v1

where the atomic dispersion is irregular [15,33]. Since the deposition of cerium in grain boundary causes finer-grained microstructure of the β-NiAl and δ-Ni2Al3 phases resulting in changing the mechanism of aluminum oxide and nickel oxide formation. XRD analysis was applied to study the major phase of the outer surface layer of coatings.

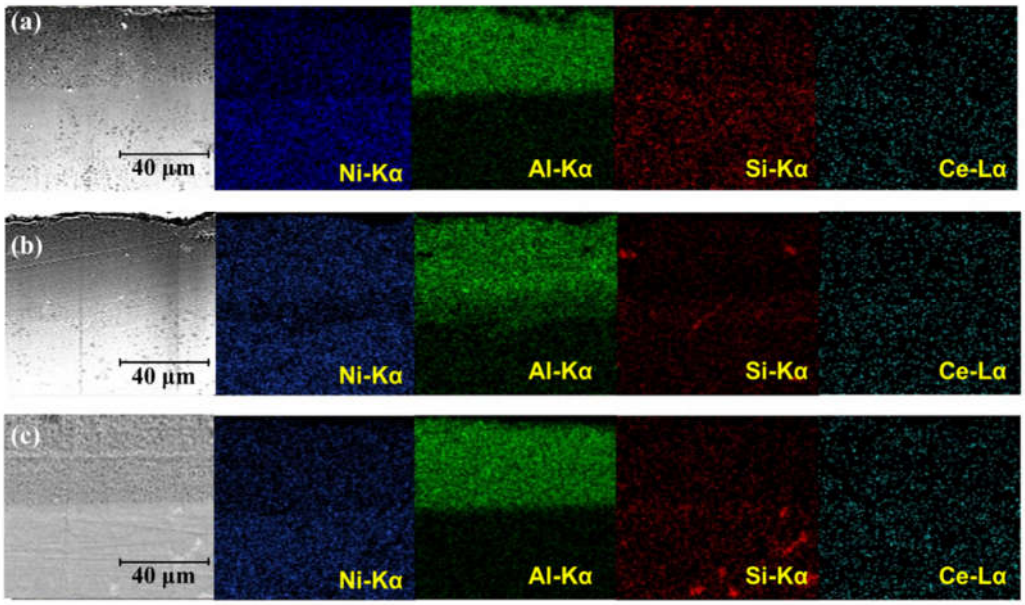

Figure 3. Elemental distribution mapping of Ni, Al, Si, Ce in a) Ce0Si3, b) Ce1Si0, c) Ce1Si6.

As can be seen from Fig. 4, the major phases of all samples are β-NiAl and δ-Ni_2Al_3. According to relative peak intensities, the δ-Ni_2Al_3 phase is dominant in the sample without cerium (Ce0Si3) compared to Ce1Si0 and Ce1Si6. In other words, the β-NiAl ratio is increased as cerium increases by 1%. This indicates that a 1% addition of cerium slightly increases the outward diffusion of nickel into the outer zone compared to the inward diffusion of Al which results in the formation of the β-NiAl phase. In the sample without silicon (Ce1Si0), there are only β-NiAl and δ-Ni2Al3 phases while δ-Ni2Si is formed as the silicon ratio is increased by 3%. This indicates that the silicon deposit was mostly present in the solid solution of β-NiAl and δ-Ni2Al3. Additionally, It can be concluded that silicon deposited is present in the form of NiAl1-nSin and Ni2Al3-nSin [22,53]. It is noteworthy that the intensity of the Ni2Si phase is increased from Ce0Si3 to Ce1Si6 sample According to the following relation (equations 1-3). In other words, the addition of silicon up to 6% increases the amount of Ni2Si formation leading to more resistance of the coating against hot oxidation [36].

$$Al+Ni \rightarrow \beta\text{-}NiAl \quad (1)$$

$$3Al+2Ni \rightarrow Ni_2Al_3 \quad (2)$$

$$[Si]+2Ni \rightarrow \delta Ni_2Si \quad (3)$$

Preprints (www.preprints.org) | NOT PEER-REVIEWED | Posted: 6 September 2022 doi:10.20944/preprints202209.0081.v1

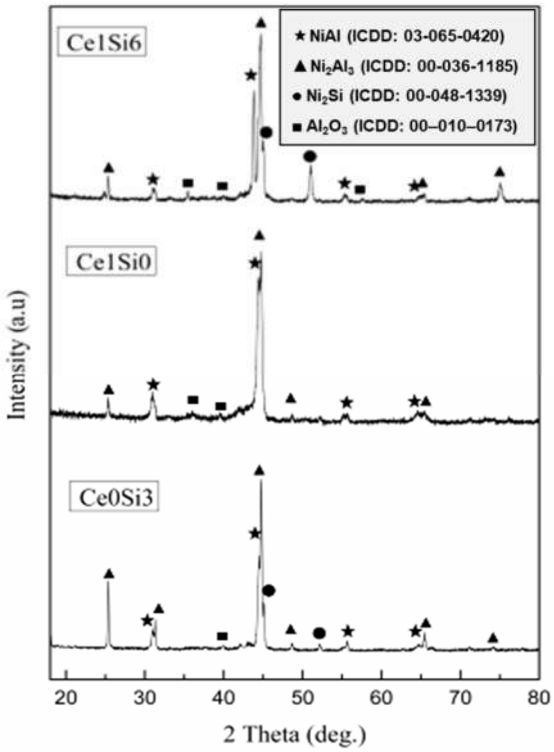

Figure 4. X-ray diffraction pattern of samples coated by pack cementation method at 1000˚C.

3.2. High-temperature oxidation

As seen in Fig. 5a, the effect of cerium content is examined on silicon-modified aluminide coating. The samples containing cerium undergo a fast weight increase earlier which is attributed to the high tendency of cerium towards oxidation. In Ce2Si3, an abrupt increase of mass gain just after 48 h oxidation is reported regarding the high ratio of cerium ion. The high ratio of cerium in the Ce2Si3, the cerium which is diffused into the β-NiAl and δ-Ni2Al3 phases increases the lattice energy of the system by lattice distortion and exfoliation of the coating [33]. As seen in Fig. 5a, the lowest weight loss and highest hot oxidation resistance are observed in the Ce1Si3 sample containing cerium 1% [9]. The weight increase of Ce1Si3 is higher compared to Ce0Si3 at the beginning of the oxidation test. Regarding the high oxidation tendency of cerium, it reacts with diffused oxygen which is diffused along the grain boundary.

Preprints (www.preprints.org) | NOT PEER-REVIEWED | Posted: 6 September 2022 doi:10.20944/preprints202209.0081.v1

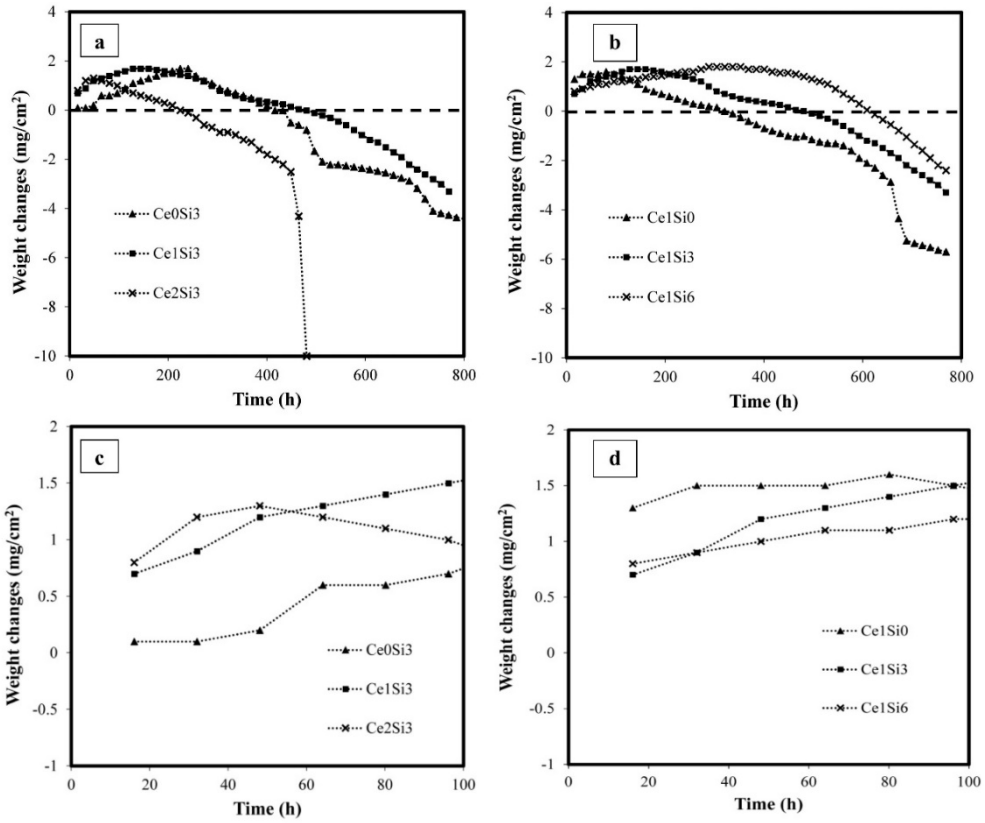

Figure 5. Cyclic high-temperature oxidation of Ce-Si-modified aluminide coatings at 1100 ˚C for 800 h. a) for samples Ce0Si3, Ce1Si3, and Ce2Si3, b) for samples Ce1Si0, Ce1Si3, and Ce1Si6, and c) and d) shows the beginning of the oxidation test in detail.

Then, cerium deposits as CeO_2 nanoparticles in the near-surface zone, and hence a higher weight increase is observed at first 160 h of high-temperature oxidation [45]. As oxidation continues, The precipitated CeO_2 fine particles located in the grain/phase boundaries could play the role of diffusion barrier and suppress the subsequent scale-up diffusion of nickel, aluminum, and silicon elements [40,54]. Also, the $Ce1Si_3$ and Ce1Si0 with finer-grained microstructure change the mechanism of aluminum oxide and nickel oxide formation and improve the adhesion of the alumina scale on the coating [43-45,55]. The samples containing 1% cerium with 0, 3, and 6% silicon were considered to study the effect of silicon on oxidation rate (Fig. 5b). A weight increase was reported in samples that could be attributed to oxygen diffusion into the system and the inception of the oxidation layer. A significant weight loss is observed after 160 h showing low resistance of Ce1Si0 coating compared to samples containing silicon. As silicon increased to 3%, the weight increase is dropped and no notable weight loss was reported until 256 h indicating an improvement in hot oxidation resistance. As the silicon ratio increases to 6%, the weight increase is slighter, and notable weight loss happened after 560 h in the hot oxidation test. It also shows that the Ce1Si6 coating shows 3.5 times higher oxidation resistance compared with to Ce1Si0 coating. Strictly speaking, alumina scale adhesion can be greatly improved by adding a small amount of cerium into the coating [56] and according to Eq. 4, the presence of silicon can prevent the oxygen inward diffusion with the formation of a protective surface scale and retard oxidation resulting in improvement of resistance of the hot oxidation [36].

$$\delta\text{-}Ni_2Si+O_2 \rightarrow 2NiO+[Si] \quad (4)$$

Preprints (www.preprints.org) | NOT PEER-REVIEWED | Posted: 6 September 2022 doi:10.20944/preprints202209.0081.v1

3.3. Characterization of oxide scale

The phases formed after 50 cycles of oxidation in the oxide layer were characterized through XRD analysis as shown in Fig. 6. As can be seen, the uniform and continuous oxide scale (α-Al_2O_3 phase) were observed in all cases of coated samples. Also, for the case of the Ce1Si6 and Ce1Si0 coatings containing 1% of cerium, the cerium oxide phase is slightly observed in those diffraction patterns. Additionally, in Ce1Si6 and Ce0Si3 coatings, a considerable amount of δ-Ni_2Si phase is converted to the Al2SiO5 phase. It is noteworthy that the SiO2 phase cannot be observed while the Al_2SiO_5 phase was detected. Also, the Si contents in the hot oxidation process accelerate the conversion of γ/-Ni_3Al to β-NiAl.

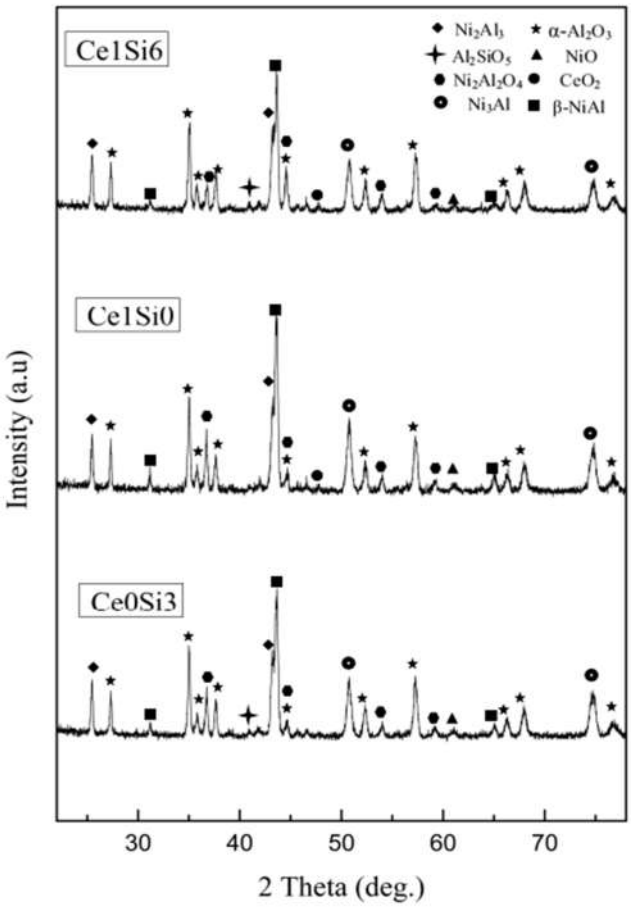

Figure 6. X-ray diffraction of coated samples after 50 cycles of oxidation tests at 1100°C.

To clarify the difference in the oxidation performance of coatings, surface morphologies of the coatings were investigated in Fig. 7. As can be seen, Ce1Si6 (Fig. 7b) shows finer morphology and less porosity compared to the oxidized Ce1Si0 (Fig. 7a) and Ce0Si3 (Fig. 7c) coatings. For the case of Ce1Si6 coating, it can be seen clearly that the grain size and volumetric fraction of NiO (bright contrast in Fig. 7b) were further reduced. Also, the α-Al2O3 appears homogeneous and uniform with less porosity in most other areas (dark areas in Fig. 7b). This implies that the fine-grained microstructure of the β-NiAl, δ-Ni2Al3 as well as cerium ions sediment in the grain boundary results in the formation of dense and equiaxed structures [51,53]. In other words, according to other related investigations [41,52], this fact indicates that a simultaneous effect of cerium and silicon results in the formation of finer and continuous alumina compared to the hot oxidation test. As a consequence, the overall growth rate of the NiO scale was also blocked effectively by the segregation of cerium to its grain boundaries [53,55,56].

Preprints (www.preprints.org) | NOT PEER-REVIEWED | Posted: 6 September 2022 doi:10.20944/preprints202209.0081.v1

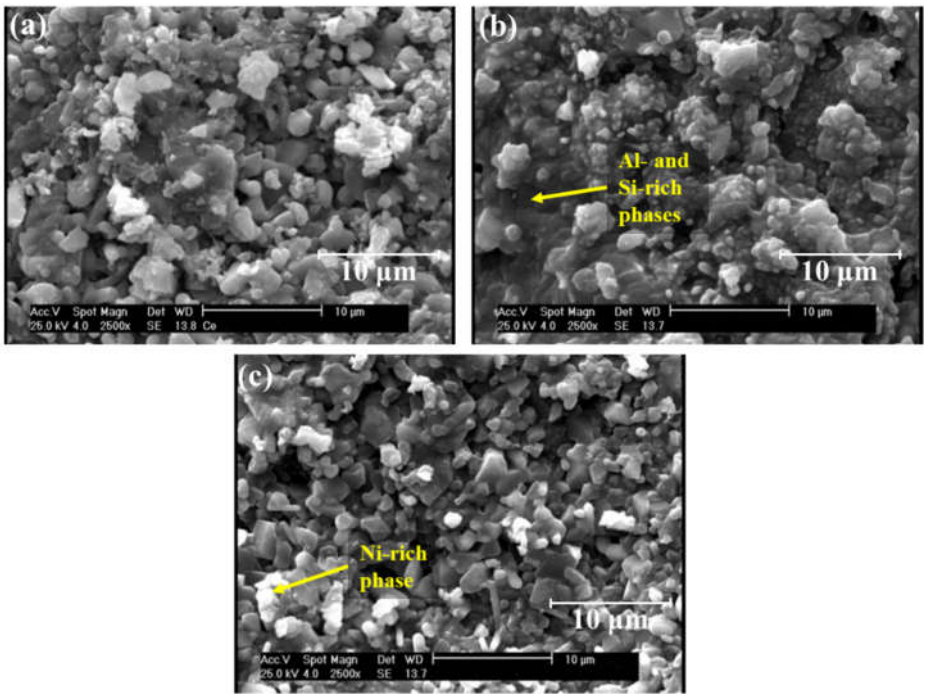

Figure 7. The surface SEM image after 50 cycles of oxidation tests at 1100°C for a) Ce1Si0, b) Ce1Si6, c) Ce0Si3.

Schematics representing the mechanism related to the oxide scale formation for the aluminide coating with and without Si and Ce addition have been shown in Fig. 8. As can be observed, there are considerable amounts of diffusion paths available for the aluminide coating containing Si owing to the dispersion of Si-ions into the grains/structure of the coating (due to the lower ionic radius of Si-ions), especially through the grain boundaries [42,43]. By this, metallic ions with higher mobility (e.g., Ni- or Al-ion) depending on their ionic activity, can diffuse easier toward the surface to form a thicker oxide scale during the cyclic test (Fig. 8a). In contrast, for Ce-Si modified aluminide coating containing both Si- and Ce-ions, even the finer structure, because of the suitable distribution of the Si-ions into the grains and concentration of Ce-ions through grain-boundaries (owing to the higher ionic radius for Ce-ion), the diffusion paths have been extensively decreased. Thus, the outward diffusion of metallic Ni- and Al-ions was sensitively limited during cyclic oxidation testing (Fig. 8b). Therefore, the growth rate of the oxide layer was decreased and so the cyclic oxidation resistance was accordingly enhanced for Ce-Si modified aluminide coating due to the synergistic effect of Si- and Ce-ions to decrease diffusion of metallic ions to form oxide scale on the coating surface [43].

Preprints (www.preprints.org) | NOT PEER-REVIEWED | Posted: 6 September 2022 doi:10.20944/preprints202209.0081.v1

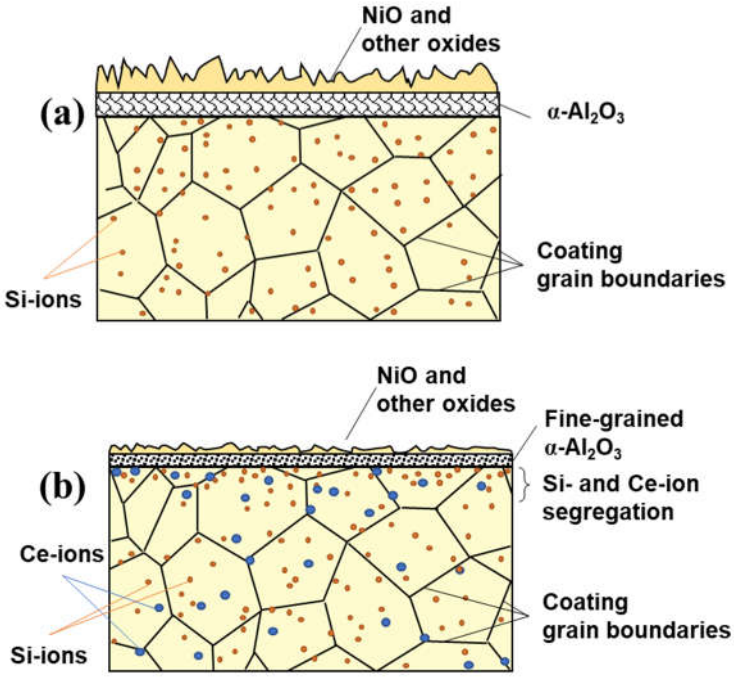

Figure 8. Mechanism of the oxide scale formation for a) aluminide coating containing Si and b) alumina coating containing both Si and Ce after cyclic oxidation test at 1100˚C for 50 cycles.

5. Conclusions

The synergistic effect of silicon and cerium on the oxidation resistance of aluminide pack cementation coating of nickel-based superalloy was investigated. Microstructure evolution of the coatings was investigated before and after the cyclic oxidation test at 1100 ˚C. The conclusion can be drawn as follows:

1. The cerium addition by 1% enhances the oxidation resistance while the oxidation resistance is limited by increasing the cerium ratio exceeding 2%. This occurs through increasing the ratio of NiAl to Ni_2Al_3, inhibiting the outward/inward diffusion of intermetallic elements and oxygen called the blocking effect in the hot oxidation process and promoting finer-grained microstructure of the NiAl and Ni2Al3 phases in the coating.
2. Increasing the cerium ratio up to 2% strictly decreases the oxidation resistance and a noticeable weight loss was observed after 450 h which is mainly attributed to cerium placed into the solid solution increasing the energy of the system by distortion and mismatch of β-NiAl and Ni_2Al_3 lattice.
3. Silicon deposited is mainly present in the form of NiAl1-nSin and Ni_2Al_3-nSin and δ-Ni_2Si in the coatings. The reaction of δ-Ni_2Si with oxygen forms active silicon atoms, and the silicon contents promote the transformation of γ′-Ni_3Al into β-NiAl and Al which improves the hot oxidation resistance of the coatings.
4. Simultaneous addition of 1% cerium and 6% silicon, Ce1Si6 sample, limits the oxygen diffusion, and can synergistically promote the formation of the continuous Al_2O_3 layer which can enhance the hot oxidation resistance of the coating.

References

1. S. Bose, Preface, in High Temperature Coatings, S. Bose, Editor., Butterworth-Heinemann Burlington. 2007 p. xi-xii.
2. Z. Xu, Z. Wang, J. Niu, L. He, R. Mu, K. Wang, Effects of deposition temperature on the kinetics growth and protective properties of aluminide coatings. Journal of Alloys and Compounds, 2015. 632: p. 238-245.
3. Z. Xu, J. Dai, J. Niu, L. He, R. Mu, Z. Wang, Isothermal oxidation and hot corrosion behaviors of diffusion aluminide coatings deposited by chemical vapor deposition. Journal of Alloys and Compounds, 2015. 637(Supplement C): p. 343-349.
4. X. Montero, M.C. Galetz, M. Schütze, Low-activity aluminide coatings for superalloys using a slurry process free of halide activators and chromates. Surface and Coatings Technology, 2013. 222: p. 9-14.
5. R. Rajendran, Gas turbine coatings – An overview. Engineering Failure Analysis, 2012. 26: p. 355-369.

6. G.W. Goward, Progress in coatings for gas turbine airfoils. Surface and Coatings Technology, 1998. 108–109: p. 73-79.
7. D.C. Dimitra Kourtidou, Christos Vogiatzis, Evangelia Tarani, Aikaterini Kamou, Eleni Pavlidou, Stefanos Skolianos, Konstantinos Chrissafis, George Vourlias, Deposition of Ni-Al coatings by pack cementation and corrosion resistance in high temperature and marine environments. 2018.
8. Marta Kianicováa, Ján Kafríka, Jaroslav Trník, Degradation of aluminide coatings deposited on nickel superalloys. Procedia Engineering, 2018.
9. M.J. Pomeroy, Coatings for gas turbine materials and long term stability issues. Materials & Design, 2005. 26(3): p. 223-231.
10. X.Z. Yuhua Zhoua, ∗, Chunshan Zhaoa, Wei Haoa, Xin Wanga,c, Ping Xiaob, The oxidation performance for Zr-doped nickel aluminide coating by composite electrodepositing and pack cementation. corrosion science, 2017.
11. Y. Chen, X. Zhao, P. Xiao, Effect of microstructure on early oxidation of MCrAlY coatings. Acta Materialia, 2018. 159: p. 150-162.
12. R. Bianco, R.A. Rapp, Pack Cementation Aluminide Coatings on Superalloys: Codeposition of Cr and Reactive Elements. Journal of The Electrochemical Society, 1993. 140(4): p. 1181-1190.
13. M.Z. Alam, S.B. Sarkar, D.K. Das, Refurbishment of thermally degraded diffusion Pt-aluminide (PtAl) bond coat on a Ni-base superalloy. Surface and Coatings Technology, 2018. 354: p. 101-111.
14. J.R. Nicholls, K.A. Long, N.J. Simms, 4.05 - Diffusion Coatings, in Shreir's Corrosion, B.C.G.L.L.R.S. Stott, Editor., Elsevier Oxford. 2010 p. 2532-2555.
15. Z. Liu, X. Zhao, C. Zhou, Improved hot corrosion resistance of Y-Ce-Co-modified aluminide coating on nickel base superalloys by pack cementation process. Corrosion Science, 2015. 92: p. 148-154.
16. H. He, Z. Liu, W. Wang, C. Zhou, Microstructure and hot corrosion behavior of Co-Si modified aluminide coating on nickel based superalloys. Corrosion Science, 2015. 100: p. 466-473.
17. Q.X. Fan, X. Peng, H.J. Yu, S.M. Jiang, J. Gong, C. Sun, The isothermal and cyclic oxidation behaviour of two Co modified aluminide coatings at high temperature. Corrosion Science, 2014. 84: p. 42-53.
18. H. Ahmadi, D.Y. Li, Mechanical and tribological properties of aluminide coating modified with yttrium. Surface and Coatings Technology, 2002. 161(2–3): p. 210-217.
19. Y.B. Zhou, H.J. Zhang, Preparation and oxidation of an Al2O3-modified aluminide coating. Vacuum, 2012. 86(9): p. 1353-1357.
20. Y. Wang, M. Suneson, Oxidation behavior of Hf-modified aluminide coatings on Haynes-188 at 1050°C. Surface and Coatings Technology, 2013. 215: p. 7-15.
21. Y. Wang, M. Suneson, G. Sayre, Synthesis of Hf-modified aluminide coatings on Ni-base superalloys. Surface and Coatings Technology, 2011. 206(6): p. 1218-1228.
22. Z.D. Xiang, P.K. Datta, Codeposition of Al and Si on nickel base superalloys by pack cementation process. Materials Science and Engineering: A, 2003. 356(1–2): p. 136-144.
23. R. Streiff, D.H. Boone, Corrosion resistant modified aluminide coatings. Journal of Materials Engineering, 1988. 10(1): p. 15-26.
24. L. Qian, F. Xu, K.T. Voisey, V. Nekouie, Z. Zhou, V.V. Silberschmidt, X. Hou, Incorporation and evolution of ZrO2 nano-particles in Pt-modified aluminide coating for high temperature applications. Surface and Coatings Technology, 2017. 311: p. 238-247.
25. S.A. Azarmehr, K. Shirvani, M. Schütze, M. Galetz, Microstructural evolution of silicon-platinum modified aluminide coatings on superalloy GTD-111. Surface and Coatings Technology, 2017. 321(Supplement C): p. 455-463.
26. Z.D. Xiang, P.K. Datta, Formation of Hf- and W-modified aluminide coatings on nickel–base superalloys by the pack cementation process. Materials Science and Engineering: A, 2003. 363(1–2): p. 185-192.
27. J. Ma, S.M. Jiang, H.Q. Li, W.X. Wang, J. Gong, C. Sun, Microstructure and oxidation behaviour of an AlSiY/NiCrAlYSi composite coating at 1150 °C. Corrosion Science, 2011. 53(4): p. 1417-1423.
28. J. Klöwer, U. Brill, U. Heubner, High temperature corrosion behaviour of nickel aluminides: effects of chromium and zirconium. Intermetallics, 1999. 7(10): p. 1183-1194.
29. H. Guo, D. Li, L. Zheng, S. Gong, H. Xu, Effect of co-doping of two reactive elements on alumina scale growth of β-NiAl at 1200 °C. Corrosion Science, 2014. 88: p. 197-208.
30. Z. Liu, X. Zhao, H. Guo, C. Zhou, Cyclic oxidation resistance of Ce/Co modified aluminide coatings on nickel base superalloys. Corrosion Science, 2015. 94: p. 135-141.
31. J.W. Yongdong Wang∗, Haiting Hu, Junsheng Meng, Xia Zhao, Effect of Y2O3 content in the pack mixtures on the cyclic-oxidation of Y2O3-modified low temperature aluminide coatings on 309 stainless steel. vaccum, 2018.
32. Z. Haijun, S. Jianfeng, Fabrication and Cyclic Oxidation of Y2O3/CeO2-Modified Low Temperature Aluminide Coatings. Rare Metal Materials and Engineering, 2017. 46(2): p. 301-306.
33. Z. Liu, X. Zhao, C. Zhou, Improved hot corrosion resistance of Y–Ce–Co-modified aluminide coating on nickel base superalloys by pack cementation process. Corrosion Science, 2015. 92: p. 148-154.
34. H. Li, M. Qiao, C. Zhou, Formation and cyclic oxidation resistance of Hf–Co-modified aluminide coatings on nickel base superalloys. Materials Chemistry and Physics, 2014. 143(3): p. 915-920.
35. A. Firouzi, K. Shirvani, The structure and high temperature corrosion performance of medium-thickness aluminide coatings on nickel-based superalloy GTD-111. Corrosion Science, 2010. 52(11): p. 3579-3585.
36. C. Fu, W.K. Kong, G.H. Cao, Microstructure and oxidation behavior of Al + Si co-deposited coatings on nickel-based superalloys. Surface and Coatings Technology, 2014. 258: p. 347-352.

37. H.W. Grünling, R. Bauer, The role of silicon in corrosion-resistant high temperature coatings. Thin Solid Films, 1982. 95(1): p. 3-20.
38. T.A. Kircher, B.G. McMordie, A. McCarter, Performance of a silicon-modified aluminide coating in high temperature hot corrosion test conditions. Surface and Coatings Technology, 1994. 68–69: p. 32-37.
39. Z.D. Xiang, P.K. Datta, Deposition of silicon modified aluminide coatings on nickel base superalloys by pack cementation process. Materials Science and Technology, 2003. 19(7): p. 935-942.
40. J.-s. Meng, Z.-s. Ji, Effect of La2O3/CeO2 particle size on high-temperature oxidation resistance of electrodeposited Ni–La2O3/CeO2 composites. Transactions of Nonferrous Metals Society of China, 2014. 24(11): p. 3571-3577.
41. Y.B. Zhou, G.G. Zhao, H.J. Zhang, Y.C. Zhang, B.Y. Qian, Effect of CeO2 on the microstructure and isothermal oxidation of Ni–Al alloy coatings transformed from electrodeposited Ni–Al films at 800°C. Vacuum, 2009. 83(11): p. 1333-1339.
42. X. Tan, X. Peng, F. Wang, The mechanism for self-formation of a CeO2 diffusion barrier layer in an aluminide coating at high temperature. Surface and Coatings Technology, 2013. 224: p. 62-70.
43. B. Bouchaud, B. Rannou, F. Pedraza, Slurry aluminizing mechanisms of Ni-based superalloys incorporating an electrosynthesized ceria diffusion barrier. Materials Chemistry and Physics, 2013. 143(1): p. 416-424.
44. Y.B. Zhou, H.T. Hu, H.J. Zhang, Oxidation behavior of aluminide coatings on carbon steel with and without electrodeposited Ni–CeO2 film by low-temperature pack cementation. Vacuum, 2011. 86(2): p. 210-217.
45. X. Peng, Y. Guan, Z. Dong, C. Xu, F. Wang, A fundamental aspect of the growth process of alumina scale on a metal with dispersion of CeO2 nanoparticles. Corrosion Science, 2011. 53(5): p. 1954-1959.
46. M. Safari, F. Shahriari Nogorani, Formation mechanism of high activity aluminide coating on Ni-CeO2 coated Rene 80 alloy. Surface and Coatings Technology, 2017. 329(Supplement C): p. 218-223.
47. Q.Z. HongyuWang ∗, HanWang, Wanli Cui, Xiaoming Yuan, Micromechanism characteristics ofmodified Al-Si coating by lasermelt injection CeO2 nano-particles. Surface & Coatings Technology, 2017.
48. Y. Saito, B. Önay, Improvements of scale adherence on heat-resisting alloys and coatings by rare earth additions. Surface and Coatings Technology, 1990. 43–44, Part 1: p. 336-346.
49. Z. Liu, C. Zhou, Hot Corrosion Behavior of Si–Y–Co-Modified Aluminide Coating Exposed to NaCl + Na2SO4 Salt at 1173 K. Oxidation of Metals, 2016. 85(1): p. 205-217.
50. M. Fukumoto, A. Yokobori, M. Hara, Formation of the β-NiAl Containing Hf by the Simultaneous Electrodeposition of Al and Hf using a Molten-Salt and the Cyclic Oxidation Behavior. Oxidation of Metals, 2016. 85(1): p. 17-28.
51. B.A. Pint, J.A. Haynes, T.M. Besmann, Effect of Hf and Y alloy additions on aluminide coating performance. Surface and Coatings Technology, 2010. 204(20): p. 3287-3293.
52. G.W. Goward, L.W. Cannon, Pack Cementation Coatings for Superalloys: A Review of History, Theory, and Practice. Journal of Engineering for Gas Turbines and Power, 1988. 110(1): p. 150-154.
53. X. M. Pan, Z. P. Jin, J.-C. Zhao, Determination of the isothermal sections of the AlNiSi ternary system at 750 °C and 850 °C. Vol. 36.2005, p.
54. H.-j. Zhang, Y.-b. Zhou, J.-F. Sun, Preparation and oxidation behaviour of electrodeposited Ni–CeO2 nanocomposite coatings. Transactions of Nonferrous Metals Society of China, 2013. 23(7): p. 2011-2020.
55. J. Romanowska, J. Morgiel, M. Zagula-Yavorska, J. Sieniawski, Nanoparticles in hafnium-doped aluminide coatings. Materials Letters, 2015. 145: p. 162-166.
56. X. Tan, X. Peng, F. Wang, The effect of grain refinement on the adhesion of an alumina scale on an aluminide coating. Corrosion Science, 2014. 85: p. 280-286.